Journal of Computer-Aided Molecular Design, 10 (1996) 177–185
ESCOM

J-CAMD 339

Molecular dynamics: Deciphering the data*

Pnina Dauber-Osguthorpe, Colette M. Maunder and David J. Osguthorpe**

Molecular Graphics Unit, School of Chemistry, University of Bath, Claverton Down, Bath BA2 7AY, U.K.

Received 8 December 1995
Accepted 16 February 1996

Keywords: Peptide; Protein; Conformational motion; Conformational searching; Normal modes; Selectively enhanced molecular dynamics; Time-domain filtering

Summary

The dynamic behaviour of molecules is important in determining their activity. Molecular dynamics (MD) simulations give a detailed description of motion, from small fluctuations to conformational transitions, and can include solvent effects. However, extracting useful information about conformational motion from a trajectory is not trivial. We have used digital signal-processing techniques to characterise the motion in MD simulations, including: calculating the frequency distribution, applying filtering functions, and extraction of vectors defining the characteristic motion for each frequency in an MD simulation. We describe here some typical results obtained for peptides and proteins. The nature of the low-frequency modes of motion, as obtained from MD and normal mode (NM) analysis, of Ace-$(Ala)_{31}$-Nma and of a proline mutant is discussed. Low-frequency modes extracted from the MD trajectories of Rop protein and phospholipase A_2 reveal characteristic motions of secondary structure elements, as well as concerted motions that are of significance to the protein's biological activity. MD simulations are also used frequently as a tool for conformational searches and for investigating protein folding/unfolding. We have developed a novel method that uses time-domain filtering to channel energy into conformational motion and thus enhance conformational transitions. The selectively enhanced molecular dynamics method is tested on the small molecule hexane.

Introduction

The dynamic properties of molecules play an important role in the way they function. In particular, their conformational flexibility is important in many biological events [1]. Experimental techniques provide little information about the motion of such systems at the atomic level. Thus, theoretical methods have to be utilised to gain insight into the dynamic behaviour of molecules. The two main theoretical approaches in the investigation of molecular motion are normal mode (NM) analysis and molecular dynamics (MD). NM analysis has often been used in the interpretation of vibrational spectroscopy of small molecules [2,3]. More recently it has been extended to larger systems and applied to a few proteins [4–9]. This method partitions the overall motion into characteristic modes of motion in terms of amplitudes and frequency, and enables a visual description of these modes. It is also possible to use these modes to calculate statistical properties (e.g. average fluctuations, covariances of atomic fluctuations, etc.) and to calculate thermodynamic properties [10–12].

MD simulations give a detailed description of motion. Unlike NM analysis, this method is applicable to conformational transitions as well as small fluctuations, and can include solvent effects. The MD method has become a widely used technique and has been utilised for two major purposes. One is to elucidate the characteristic motions of the molecular system, and the other is for searching conformational space.

Although an MD trajectory contains a wealth of information about the motion of the system, extracting useful information from it about conformational motion is not trivial. Recent approaches have included calculating covariances and correlations of atomic fluctuations [13,14], projection of fluctuations onto precalculated NM and

*This paper is based on a presentation given at the 14th Molecular Graphics and Modelling Society Conference, held in Cairns, Australia, August 27–September 1, 1995.
**To whom correspondence should be addressed.

principal component analysis [15,16]. We have used digital signal-processing techniques to characterise the motion in MD simulations. These include: calculating the frequency distribution from the Fourier transforms of all the atomic trajectories; applying filtering functions to remove high-frequency bond stretches and valence-angle bending while retaining the low-frequency conformational motion [17,18]; and extraction of vectors defining the characteristic motion for each frequency in an MD simulation (analogous to NMs) [19]. We are currently applying this method to a set of peptides and proteins in order to provide a comprehensive classification of typical modes of motions and to characterise them in terms of frequency, direction and amplitude of atomic motion. Special emphasis is given to motions of secondary structure elements, and to motions linked to biological activity. The results presented here are collated from several detailed studies on peptides and proteins. These have included the study of characteristic modes of helices of various length, sequence and packing, by using the NM and MD methods. Characteristic modes extracted from MD simulations of several proteins have depicted a variety of motions ranging from loop bending to concerted motion of β-strands, single helices or bundles.

MD simulations have also been used as a tool for conformational searches, or in conjunction with X-ray or NMR to solve structures of peptides and proteins. In principle, if the MD simulation is carried out for a long enough period, the conformational space will be sampled in full. However, this approach is not very effective, since most of the time is spent in high-frequency oscillations around the same conformation, and conformational transitions are infrequent. Several approaches have been adopted in an attempt to improve the efficiency of conformational searching. A commonly used improved protocol is the simulated annealing protocol that uses high-temperature MD followed by simulations at lowered temperature [20]. Algorithms for stochastic dynamics that quench high-frequency oscillations, and thus allow longer time steps to be used, are being developed [21,22]. Focusing the initial kinetic energy into torsion angles was another attempt to enhance the conformational searching [23]. This procedure aims to bias the simulations towards fluctuations in conformational degrees of freedom (i.e., the torsions), rather than bond and valence-angle oscillations. Previous studies of conformational flexibility revealed that conformational transitions are preceded by the channelling of energy into low-frequency conformational modes of motion [24]. Thus, amplifying the amplitude of these conformational modes should result in frequently occurring transitions. We have designed a novel MD algorithm that uses time-domain filtering [25] in order to channel energy into selected modes of motion during the whole simulation. This method of selectively enhanced molecular dynamics (SEMD) can enhance specifically any type of motion by using the appropriate filtering function for the required frequency range. However, for the purpose of enhanced conformational searching, a low-pass filter is used that enhances all modes with frequencies below a cutoff value and suppresses all modes with higher frequency. The application of SEMD to a small molecule, namely hexane, will be described.

Methods

Energy functions

The calculations performed in this study are all based on a representation of the molecules as fully flexible. The potential energy of the system is represented by an analytical function of internal coordinates and interatomic distances. The parameters for this function were refined to reproduce experimental data for a set of model compounds, including functional groups that occur in amino acids [26–28].

Minimisations and NM analysis

Using the analytical first (and second) derivatives of the energy with respect to Cartesian coordinates, the energy of the system can be minimised to yield the equilibrium structure [29]. Normal-mode analysis was carried out by diagonalising the matrix of second derivatives of the energy with respect to the Cartesian coordinates [3]. This yields a set of eigenvectors and values that define the normal modes and frequencies. A normal mode k is described as the set of oscillations in the mass-weighted Cartesian coordinates, q_{ik}, of the atoms:

$$q_{ik}(t) = l_{ik}\cos(\nu_k t + \varepsilon_k) \quad (1)$$

where l_{ik}, ν_k and ε_k are the amplitude, frequency and phase for mode k.

MD simulations

In the molecular dynamics simulations Newton's equations of motion were solved numerically, to produce a trajectory of atomic positions, velocities and energies [30,31].

SEMD simulations

This type of simulation involves reassignment of the atomic velocities to correspond to those of modes in a selected frequency range, i.e., a time-domain filtering function is applied to the atomic velocities:

$$v_i'(t_n) = \sum_{k=0}^{M} C_k v_i(t_{n-k}) \quad (2)$$

where $v_i'(t_n)$ is the filtered velocity of atom i at time t_n.

These velocities are obtained from the set of velocities at the M previous time steps. The values of C_k define the filtering function. For the purpose of enhanced confor-

mational searching a low-pass filter is used in which all C_k values are set to one. The number of previous steps included in the filtering, M, determines the cutoff frequency. A similar filter has been used previously for interactive filtering of the coordinates in MD trajectories [32].

Analysis of the trajectories

Frequency distribution The frequency distribution function, g(ν), gives the number of characteristic motions in the system with a frequency ν. This function is obtained from the trajectories of atomic coordinates [17,33]:

$$g(\nu_a) = (1/kT)\nu_a^2 \sum_i H_i^2(\nu_a) \tag{3a}$$

$$H_i(\nu_a) = 1/N \sum_{m=1}^{N} q_i(t_m) e^{-j\nu_a t_m/N} \tag{3b}$$

where $q_i(t_m)$ are the mass-weighted displacement coordinates and $H_i(\nu_a)$ are the corresponding Fourier transforms.

Extracting characteristic modes of motion NMs were defined in Eq. 1 in terms of frequency and atomic amplitudes. An analogous description is obtained from MD simulations using Fourier transform techniques. A sample mode, a, is defined by the set of amplitudes, I_{ia}, of all coordinates at a specific frequency, ν_a. The absolute value of I_{ia} is given by the magnitude of the Fourier transform of coordinate i at frequency point a:

$$|I_{ia}| = |H_i(\nu_a)| \tag{4a}$$

where $H_i(\nu_a)$ is defined in Eq. 3b. The relative direction is given by:

$$\begin{aligned} &\text{Sign}[I_{ia}] = \text{sign}[\text{Real}[H_i(\nu_a)] \\ &\text{for Real}[H_i(\nu_a)] > \text{Imag}[H_i(\nu_a)] \\ &\text{Sign}[I_{ia}] = \text{sign}[\text{Imag}[H_i(\nu_a)] \\ &\text{for Real}[H_i(\nu_a)] < \text{Imag}[H_i(\nu_a)] \end{aligned} \tag{4b}$$

For further details see Ref. 19.

Characterisation of extracted and normal modes

One of the most effective ways to convey the nature of a mode is by constructing a vector representation to be displayed along with the molecule. For each atom a vector is shown that originates from the equilibrium position, points in the direction of motion and its size is proportional to the atomic amplitude. Along with this representation, it is also useful to display a matrix of covariances or cross-correlations of atomic fluctuations. In addition, the representation of the modes could be transformed from Cartesian coordinates to other systems, such as internal coordinates, or in a coordinate system along a helical secondary structure unit with axial, radial and tangential components.

Results

Isolated helices

The two systems compared here are oligopeptides blocked by acetyl and *N*-methyl amide groups. The first helix is an alanine homo-oligopeptide, Ace-$(Ala)_{31}$-Nma (A31) and the other is Ace-$(Ala)_{21}$-Pro-$(Ala)_9$-Nma (A22P). The helices were built using standard geometry and conformation. These initial structures were then fully minimised. This was followed by NM analysis and 165 ps of MD simulation at 300 K. The low-frequency modes in the period 102–135 ps were extracted using digital signal techniques (Eq. 4). Thus, both methods resulted in vectors (and associated frequencies) describing the motion of each atom for the various modes. The degree of similarity between the modes obtained by the two methods is given by their dot product, and is shown in Fig. 1. The frequency distribution g(ν) during this time period in the MD trajectory is presented in Fig. 1 above the similarity matrices. The three lowest normal modes of A31 and A22P are shown on the left in Figs. 2A and B, respectively. The MD mode corresponding to the highest g(ν) for the two oligopeptides is shown on the right. For each of these modes the matrix of residue–residue covariances is also shown.

Rop protein

The crystal structure of ColE1 Rop protein was used as the initial structure [34]. All hydrogen atoms were added to the four-helix bundle, water molecules and counterions were added and the system was minimised using periodic boundary conditions. An MD simulation with twin temperature baths at 300 K was carried out for 350 ps. The simulation converged after ≈ 110 ps, and the time period 120–202 ps was used for the analysis presented here (this corresponds to a frequency resolution of 0.4 cm^{-1}). Figure 3 depicts some of the typical motions extracted from the MD trajectory. The sample mode at 2.0 cm^{-1} reveals a twisting motion for the N-terminal section of helix A. The axial and lateral components of the sample mode at 4.9 cm^{-1} are depicted in Figs. 3B and C, respectively.

Phospholipase A_2

The experimental structure of bovine phospholipase A2 was used as the initial structure [35]. Hydrogen atoms and water molecules were added and the system was minimised using periodic boundary conditions. An MD simulation at 300 K was carried out for 70 ps. Convergence was achieved after ≈ 25 ps and the time period 27.5–68.5 ps was used for the analysis (corresponding to a frequency resolution of 0.8 cm^{-1}). Figure 4A depicts the concerted motion of helices C and E, which carry the catalytic couple His^{48} and Asp^{99} (frequency of 3.3 cm^{-1}). Figure 4B shows the relative motion of the residues at the entrance to the active site (frequency of 1.6 cm^{-1}).

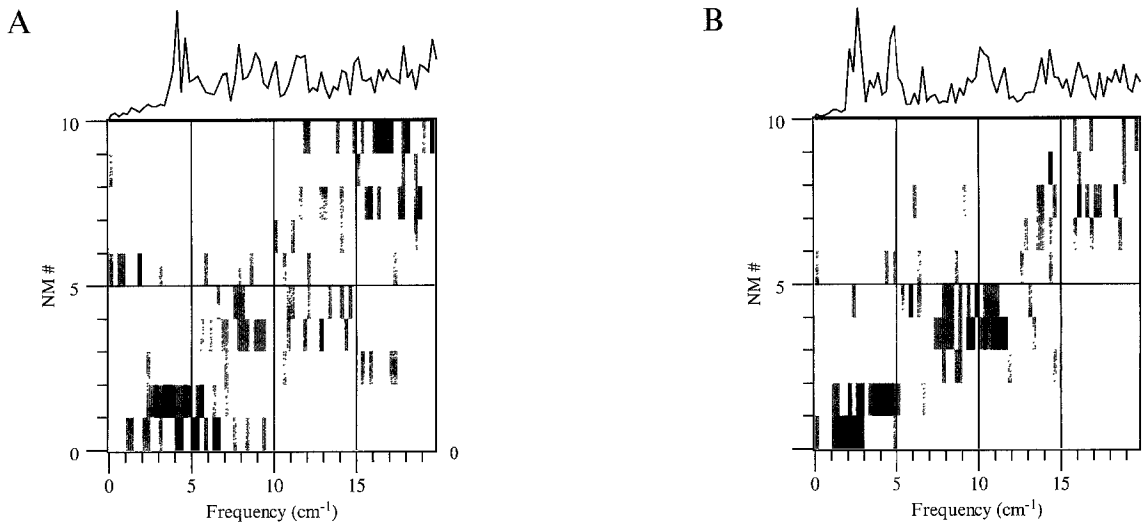

Fig. 1. Comparison of normal modes and modes extracted from MD trajectories for: (A) alanine homo-oligopeptide (A31); and (B) proline mutant (A22P). The corresponding frequency distributions are given on top. High and medium correlations are shown in black and gray, respectively.

Hexane SEMD

A minimised all-trans initial conformation was used for all simulations. Three 64-ps simulations at 300 K were carried out: (i) a regular one (rMD); (ii) a simulation in which low-frequency motion is enhanced continuously (cSEMD); and (iii) a simulation with intermittent low-frequency motion enhancement (iSEMD). A window of 0.07 ps (corresponding to a maximum frequency of ~300 cm^{-1}) was used for the application of the time-domain filter. In the iSEMD simulation the filtering was carried out in 1-ps intervals interspersed with periods of 0.5-ps regular MD. For each of the trajectories the conformational degrees of freedom, i.e., the three C–C dihedral angles, were monitored. These are shown in Fig. 5. The overall frequency distribution in each of the simulations is also shown.

Discussion

Low-frequency characteristic motion of isolated helices

The typical low-frequency modes of motion of oligopeptides in the helical conformation were examined using NM analysis and by extracting characteristic modes from MD trajectories. Comparisons of the 10 lowest-frequency NMs and the extracted sample modes below 20 cm^{-1} are shown for A31 and A22P in Fig. 1. As can be seen in this figure, there is a high correlation between NMs and MD sample modes along the diagonal. This indicates that the two methods give similar descriptions of the low-frequency modes in terms of frequency ranking and direction and amplitudes of atomic motion.

Further characterisation of this typical motion is given in Fig. 2. The three lowest-frequency modes are two bends in perpendicular directions, and a twisting mode. The relative frequencies of the bending and twisting modes depend on helix length and composition (C.M. Maunder et al., unpublished results). The twisting mode is the lowest mode for short helices, but for helices longer than 18 residues the bends are lower in frequency than the twist. For A31 the frequencies of the two bends are 3.8 and 3.9 cm^{-1}, and the frequency of the twist mode is 6.1 cm^{-1}. The pattern of covariances for the two lowest modes suggests that the middle section of the helix is moving in the same direction, and both terminal sections are moving in the opposite direction. This pattern corresponds to radial motion, perpendicular to the helix axis, and is indicative of a bending motion, as born out in the vector representations of the modes. The diagonal pattern of covariances of the third mode suggests that between residue i and residues (i+1), (i+2), (i+3) and (i+4) there is no covariance, negative covariance, no covariance, and positive covariance, respectively. This pattern corresponds to motion perpendicular to the helix axis, in a direction tangential to the helix circumference, i.e., a twisting motion, as shown in the vector representation. In the fourth column of Fig. 2A the covariance matrix and vector representation of a typical MD sample mode is given. This mode corresponds to a frequency of 4.6 cm^{-1}, and has the highest g(v) (Fig. 1A) and highest amplitude. It is obvious that this is a bending mode with the same characteristics as the bending modes obtained from NM analysis.

An important characteristic property of these and other low-frequency modes is the delocalised nature of the motion. Analysis of the torsional components of each of the low-frequency modes reveals that these motions involve changes along the whole peptide chain. Even the bending mode, which superficially could be envisaged as rigid-body motion of two halves of the helix relative to a single hinge point, actually involves changes of all ϕ,ψ torsion angles.

A similar analysis was carried out for A22P. Again, the two lowest NMs are perpendicular bends, and the next

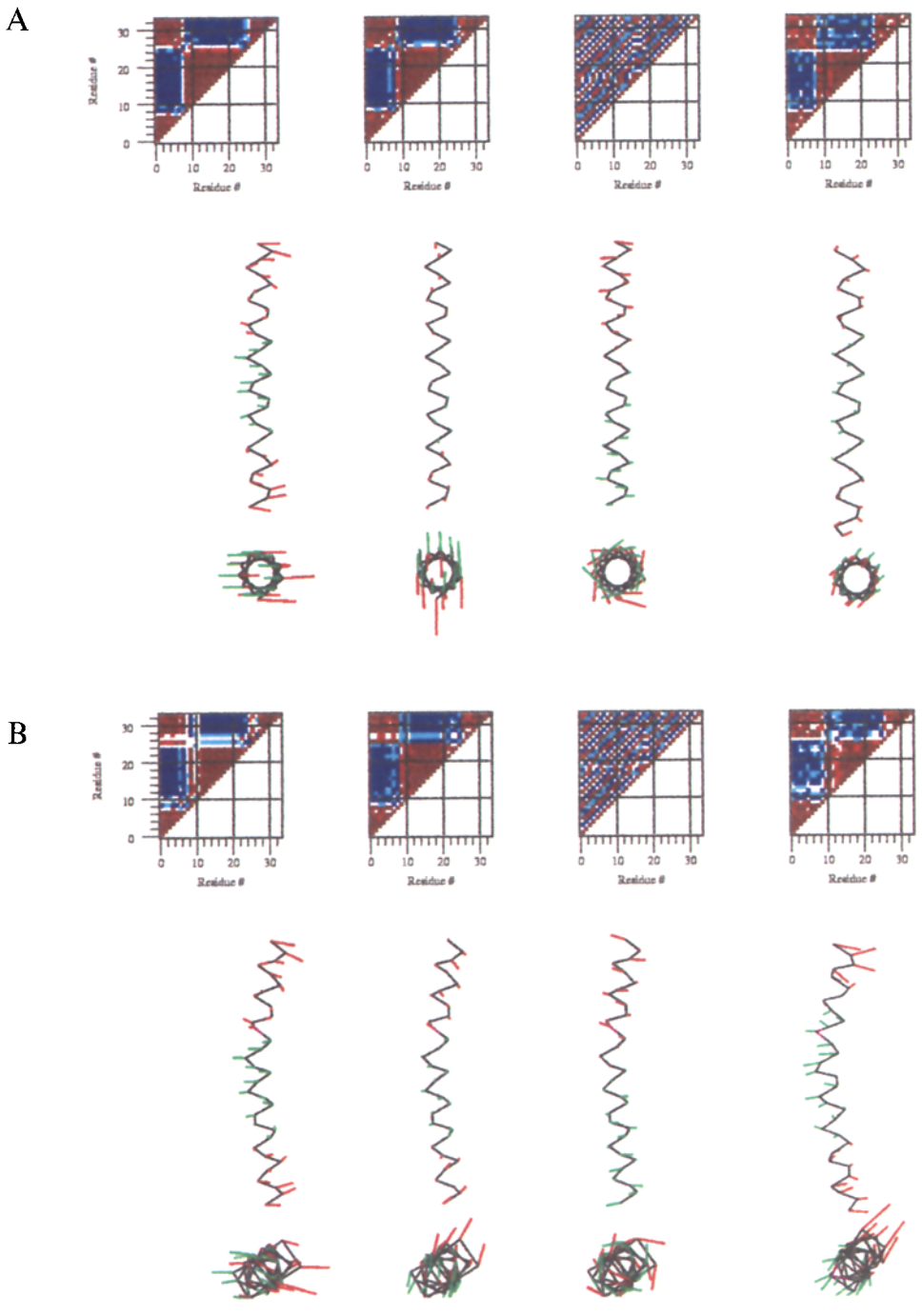

Fig. 2. Low-frequency modes of motion for: (A) alanine homo-oligopeptide (A31); and (B) proline mutant (A22P). The three lowest-frequency modes are shown from left to right in order of increasing frequency. The fourth mode was extracted from an MD trajectory. The C^{α} atoms are shown in black; the modes are shown in red and green; two perpendicular views are presented for each mode. The correlation matrices are shown on top: strong positive and negative correlations are shown in red and blue, respectively.

mode is a twist. However, the two bending modes are not degenerate, as for the A31 helix. The frequency of bending in one of the directions, 4.0 cm^{-1}, is similar to that of A31, but bending in the perpendicular direction is lowered to 3.0 cm^{-1}. A similar trend is observed in the MD simulation as well. Whereas the first peak in g(ν) for A31 is at ~4 cm^{-1}, the first peak for A22P is at ~3 cm^{-1} (see Figs. 1A and B, respectively). A larger amplitude of bending motion is concomitant with the lower frequency, due to the inverse relation between the frequency of a motion and its amplitude [36].

The direction of the bend with lowered frequency is determined by the position of the Ala → Pro mutation. Since the repeat in a helix is nearly four residues, moving the mutation by one residue changes the preferred bending direction by ≈90° (C.M. Maunder et al., unpublished

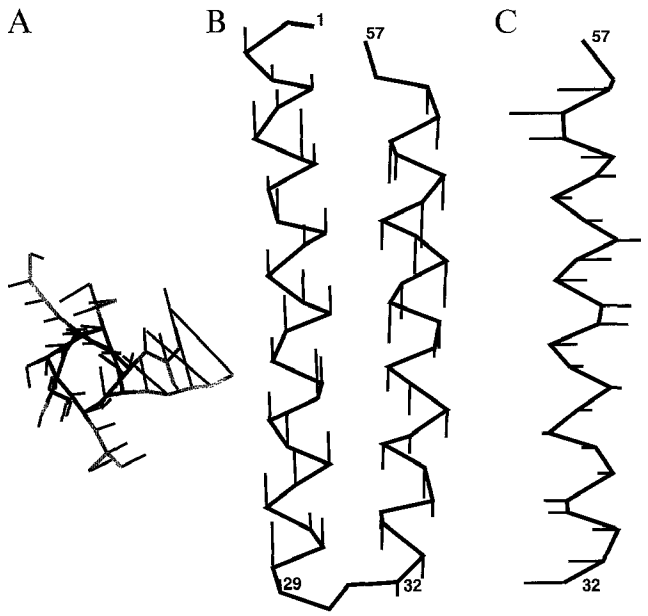

Fig. 3. Low-frequency modes of motion of Rop protein. Thick and thin lines represent the molecule and the modes, respectively. (A) Twisting motion (2.0 cm^{-1}). Backbone and side chains are shown in black and gray, respectively; (B) the axial component of an extracted mode for helices A and B (4.9 cm^{-1}); and (C) the lateral component of an extracted mode for helix B (4.9 cm^{-1}).

results). Thus, this analysis reveals that a proline residue in a helix has dynamic as well as structural implications [37]. In addition to the kink in the helical structure, the proline residue enhances the helix-bending motion, and introduces a preferred direction for bends.

Motion of protein secondary structure units

For small systems with well-defined conformations NM and modes extracted from MD provide similar information, as seen above. For large systems with at least some regions of considerable flexibility, such as proteins, MD is the only viable method. Analysis of MD trajectories of proteins reveals a range of characteristic motions. The MD trajectory of the four-helix bundle, Rop, revealed internal helix motion with similar features to those observed for isolated helices. The residue–residue covariance matrix of the sample mode corresponding to a frequency of 2 cm^{-1}, for the N-terminal end of helix A, reveals the same pattern of diagonal stripes as the twisting mode of the isolated helices in Fig. 2. The twisting nature of the motion is also evident in the vector representation in Fig. 3A. Another sample mode extracted from the MD trajectory of Rop, 4.9 cm^{-1}, has intra- and interhelix components. The major part of the motion in this mode is along the helices' axis. This component of the motion can be described as rigid-body motion of the helices. Each pair of helices in a chain moves in opposite directions in a shear motion (Fig. 3B). The adjacent helices of different chains move in the same direction. Some parts of the lateral (perpendicular to the helix axis) motion bear resemblance to motions observed for the isolated helices. For example, the lateral components of this motion for helix B (Fig. 3C) are similar to the bending motion of the oligopeptides (Fig. 2).

Analysis of the motion exhibited by other proteins with other secondary structure units reveal a range of low-frequency typical modes. Rigid-body motion of helices was observed in simulations of PLA_2 (see below) and ribonuclease H. For the first protein this motion was translational in nature, while in the second helix rotation was observed. The β-strands in ribonuclease H also exhibited concerted rigid-body motion (Calleja et al., unpublished results). The largest-amplitude low-frequency motions of the protein SGPA involved mainly surface loops (P. Dauber-Osguthorpe et al., unpublished results). Thus, a set of typical low-frequency motions emerges from the analysis of MD simulations of different proteins. However, the nature of the most prominent modes depends on the specific features of secondary structure of

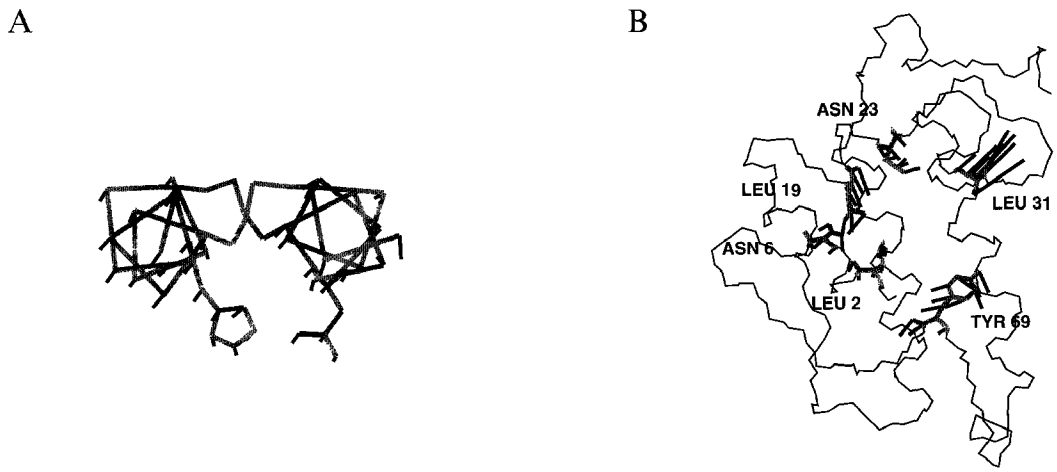

Fig. 4. Low-frequency modes of motion of phospholipase A_2. (A) Concerted motion of helices C and E. The molecule and mode of motion are shown in gray and black, respectively. (B) Motion of residues in the entrance to the active-site cavity. The backbone of the whole protein is shown in thin black lines. The relevant side chains and the vectors representing their movements are shown in thick gray and black lines.

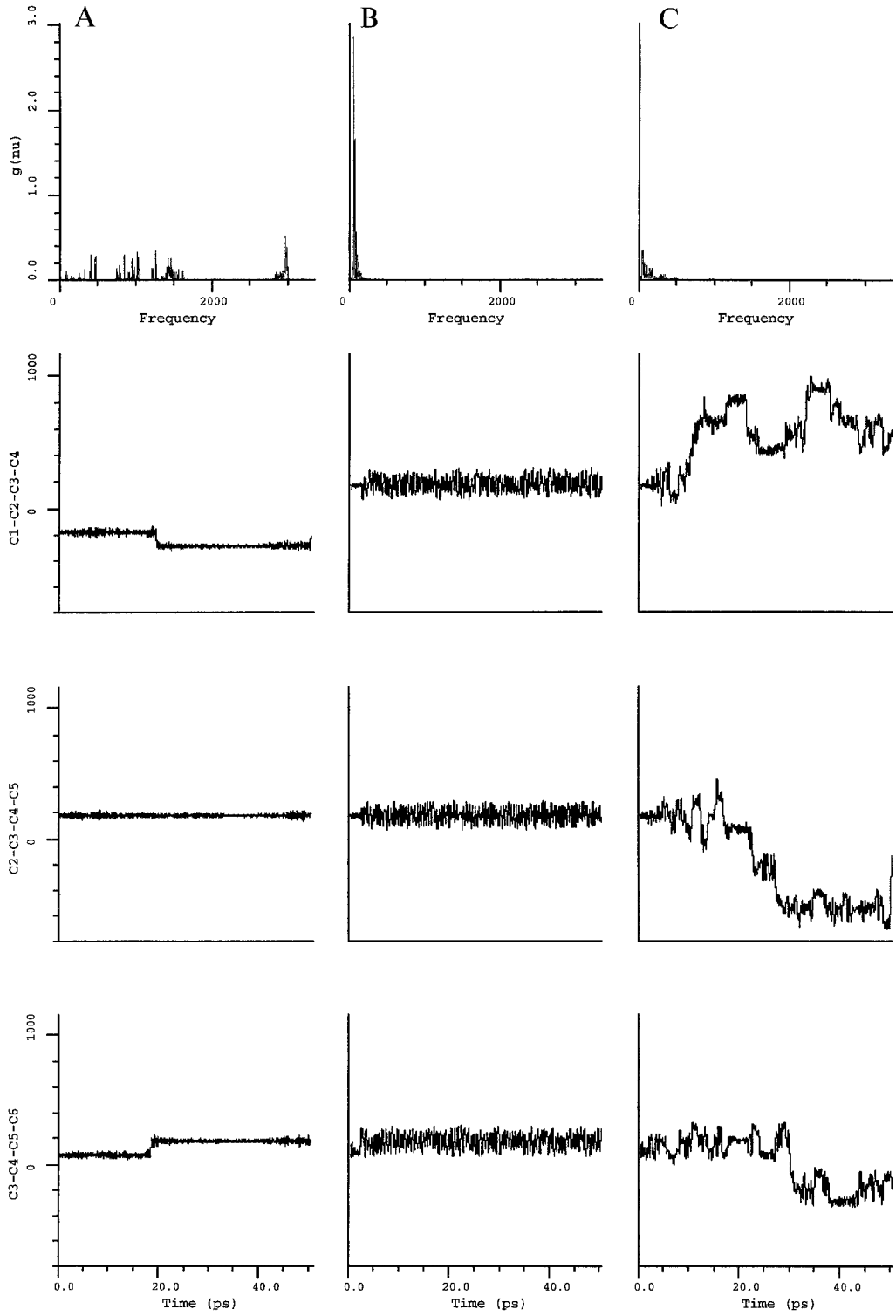

Fig. 5. SEMD of hexane. (A) Regular MD; (B) continuous SEMD; and (C) intermittent SEMD. The frequency distribution is shown in the top panel and the trajectory of the three C–C–C–C torsions is shown below. Frequencies are in cm^{-1} and torsions are in degrees.

the protein, and may be closely related to their biological activity.

Protein motion and biological activity

A study of the dynamics of the enzyme PLA_2 yields several features of motion that are closely linked to the enzyme's function. The first example is the motion of helices C and E, which include the catalytic couple His[48] and Ala[99]. It is obvious even from the average atomic fluctuations (and from the corresponding experimental

temperature factors) that these helices have relatively low mobility. However, extracting the characteristic modes of motion from the trajectory provide deeper insight into the nature of the motion. As can be seen in Fig. 4A, the central sections of these two helices move concertedly in the same direction. Thus, not only is the overall mobility of these helices low, the motion that does occur keeps the catalytic couple in contact.

Other regions of the enzyme also reveal low-frequency concerted motion. A detailed examination of low-frequency sample modes of the active-site entrance revealed concerted motion, mainly of the side-chain atoms. The residues at the entrance to the active-site cavity move in a concerted manner, changing the size and shape of the opening. The motion of six residues at the cavity entrance for the 1.6 cm^{-1} mode is depicted in Fig. 4B. The motion of these residues can be described in general as a breathing mode that opens and closes the entrance. This type of motion may be involved in the process of ligand binding, which is consistent with previous studies showing the necessity to rearrange the side chains of some of these residues in order to enable efficient binding [38].

Selectively enhanced molecular dynamics

We used hexane as a test case for applying the selectively enhanced molecular dynamics (SEMD) technique. The molecule has three C–C rotatable bonds that could adopt trans- or gauche-conformations. In regular MD, conformational transitions occur very rarely, as can be seen in Fig. 5A. During the 65-ps simulation only one trans → gauche transition occurred for the first and last C–C torsion, and none for the central C–C torsion. The frequency distribution shown in Fig. 5A at the top includes components for all typical alkane modes. The highest frequencies (~ 3000 cm^{-1}) are CH stretches; HCH stretches are at ~ 1500 cm^{-1}; HCC bends and CC stretches are in the 700–1400 cm^{-1} range, and CCC bends are in the 300–500 cm^{-1} region. The lowest-frequency modes 90–300 cm^{-1} correspond to CC torsion modes. In order to amplify the torsional motion we applied a time-domain filtering function with a maximum frequency of ~ 300 cm^{-1}. The frequency distribution of the resulting trajectory reveals that all modes above 200 cm^{-1} have been suppressed, while the modes below 150 cm^{-1} have been enhanced dramatically (Fig. 5B). This enhancement is also reflected in the torsion trajectories. The standard deviation in fluctuations were increased from ~ 10° to ~ 60°. The range of torsion values in this trajectory corresponds to both trans- and gauche-conformations. However, the filtering effectively locks the molecule into a specific motion: each of the torsions keeps oscillating between the two conformations without settling in any of the minima or continuing to further minima. A modified strategy was utilised in order to promote conformational transitions. Instead of applying the filtering function continuously, regular MD is restored at constant intervals. This enables the system to redistribute some of the energy allowing motion along new directions (consistent with the modified conformation) to develop. Thus, when filtering restarts, conformational motions in alternative directions are amplified leading to new conformational transitions. Figure 5C demonstrates the success of this strategy. Each of the three torsions undergoes many conformational transitions, with oscillations around a local minimum for very short periods between transitions. The intermisions in low-frequency-motion amplification results in a wider frequency distribution (Fig. 5C) than the one obtained for continuous amplification of low-frequency motion (Fig. 5B). However, the motion is still predominantly low-frequency motion, and seems very effective in inducing frequent conformational transitions.

Conclusions

The results presented here demonstrate the use of digital signal-processing techniques for two general purposes: to gain insight into the nature of the motion in MD trajectories and to selectively enhance specific types of motion during MD simulations.

NM analysis and extraction of modes from MD trajectories were used in order to characterise the low-frequency motion of oligopeptides in the helical conformation, in terms of frequency, atomic amplitude and direction of motion. The peptides in this conformation undergo relatively small fluctuations, and thus a similar description of the motion is obtained using both methods. Both methods suggest that for long helices the modes of lowest frequency are two degenerate bends (in perpendicular directions) and a twist. Mutating one alanine residue to a proline was found to have important dynamic implications: the frequency of one of the bends was lowered and its amplitude increased. The position of this mutation determined the relative direction of the bend.

Analysis of MD trajectories of proteins by extracting characteristic modes of motion enabled the detection of several typical low-frequency concerted modes of motion of secondary structure units. These included internal motion as well as rigid-body motion of the units as a whole. The helices in the Rop protein exhibited bends and twists similar to those observed for the isolated helices. In addition, rigid-body translational motion parallel to the helix axis also occurred. Of particular interest are extracted modes of motion, which are linked to biological activity. For example, the two helices that include the catalytic couple of phospholipase A_2 moved in a concerted manner and thus kept these two residues in close proximity. Residues in the entrance to the active site exhibited a concerted motion that opened and closed the entrance, and thus may be of importance in the process of ligand docking.

We also demonstrated the effectiveness of the SEMD method in enhancing conformational searching. By using a time-domain low-pass filtering technique, the atomic velocities were reassigned in a manner leading to low-frequency motion and suppressing high-frequency oscillations. The amplified conformational oscillations lead to a dramatic increase in the occurrence of conformational transitions. The method is extremely simple, both conceptually and in terms of ease of implementation in existing software. It does not modify the energy landscape, by fixing or stiffening some of the degrees of freedom. Instead, it guides the trajectory along favourable low-energy paths. Although channelling of energy into low-energy conformational degrees of freedom can also be done by introducing distortions in torsion angles in the initial structure, the energy gets redistributed quickly during the simulation. The SEMD method channels the energy into the required modes during the whole trajectory so that the conformational motion does not dissipate. The continuous nature of the method also ensures that the enhanced modes reflect the current conformation and environment. Whenever new conformations have been induced, the modes of motion will change accordingly and the filtering process will enhance these modified modes. Although for conformational searching applications a low-pass time-domain filter is adequate, other filters can be designed and used for investigating specific pathways for conformational transitions. Thus, the SEMD method should be a useful tool for diverse applications, such as efficient conformational searching, studies of conformational pathways and enhancing particular modes of motion that are linked to the system's activity.

Acknowledgements

This work was supported by a grant from the SERC.

References

1 Gerstein, M., Lesk, A.M. and Chotia, C., Biochemistry, 33 (1994) 6739.
2 Herzberg, G., Molecular Spectra and Molecular Structure II. Infrared and Raman Spectra of Polyatomic Molecules., D. van Nostrand Company, New York, NY, 1945.
3 Wilson, E.B., Decius, J.C. and Cross, P.C., Molecular Vibrations, McGraw Hill, New York, NY, 1955.
4 Brooks, B. and Karplus, M., Proc. Natl. Acad. Sci. USA, 80 (1983) 6571.
5 Go, N., Noguti, T. and Nishikawa, T., Proc. Natl. Acad. Sci. USA, 80 (1983) 3696.
6 Levitt, M., Sander, C. and Stern, P.S., J. Mol. Biol., 181 (1985) 423.
7 Brooks, B. and Karplus, M., Proc. Natl. Acad. Sci. USA, 82 (1985) 4995.
8 Seno, Y. and Go, N., J. Mol. Biol., 216 (1990) 95.
9 Tirion, M.M. and ben-Avraham, D., J. Mol. Biol., 230 (1993) 186.
10 Hagler, A.T., Stern, P.S., Sharon, R., Becker, J.M. and Naider, F., J. Am. Chem. Soc., 101 (1979) 6842.
11 Tidor, B. and Karplus, M., Protein Struct. Funct. Genet., 15 (1993) 71.
12 Tidor, B. and Karplus, M., J. Mol. Biol., 238 (1994) 405.
13 Ichiye, T. and Karplus, M., Protein Struct. Funct. Genet., 11 (1991) 205.
14 Amadei, A., Linssen, A.B.M. and Berendsen, H.J.C., Protein Struct. Funct. Genet., 17 (1993) 412.
15 Horiuchi, T. and Go, N., Protein Struct. Funct. Genet., 10 (1991) 106.
16 Kitao, A., Hirata, F. and Go, N., Chem. Phys., 158 (1991) 447.
17 Dauber-Osguthorpe, P. and Osguthorpe, D.J., J. Am. Chem. Soc., 112 (1990) 7921.
18 Sessions, R.B., Dauber-Osguthorpe, P. and Osguthorpe, D.J., J. Mol. Biol., 210 (1989) 617.
19 Dauber-Osguthorpe, P. and Osguthorpe, D.J., J. Comput. Chem., 14 (1993) 1259.
20 Wilson, S.R. and Cui, W., In Merz Jr., K.M. and Le Grand, S.M. (Eds.), Conformational Searching Using Simulated Annealing, in The Protein Folding Problem and Tertiary Structure Prediction, Birkhauser, Boston, MA, 1994, pp. 43–70.
21 Hao, M.-H., Pincus, M.R., Rackovsky, S. and Scheraga, H.A., Biochemistry, 32 (1993) 9614.
22 Derreumaux, P. and Schlick, T., Protein Struct. Funct. Genet., 21 (1995) 282.
23 Morley, S.D., Jackson, D.E., Saunders, M.R. and Vinter, J.G., J. Comput. Chem., 13 (1992) 693.
24 Sessions, R.B., Osguthorpe, D.J. and Dauber-Osguthorpe, P., J. Phys. Chem., 99 (1995) 9034.
25 Press, W.H., Flannery, B.P., Teukolsky, S.A. and Vetterling, W.T., In Numerical Recipes: The Art of Scientific Computing, Cambridge University Press, Cambridge, U.K., 1986.
26 Dauber-Osguthorpe, P., Roberts, V.A., Osguthorpe, D.J., Wolff, J., Genest, M. and Hagler, A.T., Protein Struct. Funct. Genet., 4 (1988) 31.
27 Hagler, A.T., Huler, E. and Lifson, S., J. Am. Chem. Soc., 96 (1974) 5319.
28 Lifson, S., Hagler, A.T. and Dauber, P., J. Am. Chem. Soc., 101 (1979) 5111.
29 Fletcher, R., Practical Methods of Optimization, 1, Wiley, New York, NY, 1980.
30 McCammon, J.A. and Harvey, S.C., Dynamics of Proteins and Nucleic Acids, Cambridge University Press, Cambridge, U.K., 1987.
31 Allen, M.P. and Tildesley, D.J., Computer Simulation of Liquids, Clarendon, Oxford, U.K., 1987.
32 Levitt, M., J. Mol. Biol., 220 (1991) 1.
33 Dauber-Osguthorpe, P., Conformation and Internal Motion of Polypeptides. Molecular Dynamics Simulations, Ph.D. Thesis, 1990.
34 Banner, A.W., Kokkinidis, M. and Tsernoglou, D., J. Mol. Biol., 196 (1987) 657.
35 Dijkstra, B.W., Kalk, K.H., Hol, W.G.J. and Drenth, J., J. Mol. Biol., 147 (1981) 97.
36 Go, N., Biophys. Chem., 35 (1990) 105.
37 Williams, K.A. and Deber, C.M., Biochemistry, 30 (1991) 8919.
38 Sessions, R.B., Dauber-Osguthorpe, P. and Osguthorpe, D.J., Protein Struct. Funct. Genet., 14 (1992) 45.